

# Second-Order Solution for Semi-Submerged Horizontal Rectangular Cylinder

By

Wojciech Sulisz

Institute of Hydroengineering, Polish Academy of Sciences, Kościarska 7, 80953 Gdańsk, Poland;  
Department of Hydraulics, Chalmers University of Technology, 41296 Göteborg, Sweden

## 1. INTRODUCTION

Many structures exposed to water wave action possess a rectangular cross-section. Ships, docks, caissons, as well as some breakwaters, belong to this group. Linear diffraction and radiation problems for such structures have been solved by applying various methods. Some second-order numerical solutions have also been published for a semi-submerged horizontal rectangular cylinder. However, most attention has focused on the mean force.

Numerical methods are recognized tools to deal with nonlinear diffraction or radiation problems. The necessity of verification of the numerical solutions, several inconsistent theoretical approaches in the published literature, and many more reasons create the need of developing other methods of solution to the nonlinear problems. Application of such a method e. g. the method of matched eigenfunction expansions at second order is one of the purposes of the present paper. The additional purpose, however, is to present and further discuss the author's theoretical result cited by Johansson (1989), which shows that the second-order components may, in deep water, become significant contributions to the loads. This conclusion has been derived for a semi-submerged horizontal rectangular cylinder. Results of a simplified theoretical approach for the calculation of the second-order vertical force acting on the horizontal rectangular cylinder by Newman (1990) and an approximate solution to the second-order boundary-value problem for a horizontal rectangular cylinder of substantial draft by Sulisz and Johansson (1992) confirm this conclusion.

## 2. THEORETICAL FORMULATION

A floating horizontal cylinder of rectangular cross-section, shown schematically in Figure 1, is considered. It is assumed that the excitation is provided by normally incident plane waves of small amplitude  $A_0$  and frequency  $\omega$ , and that the velocity has a potential.

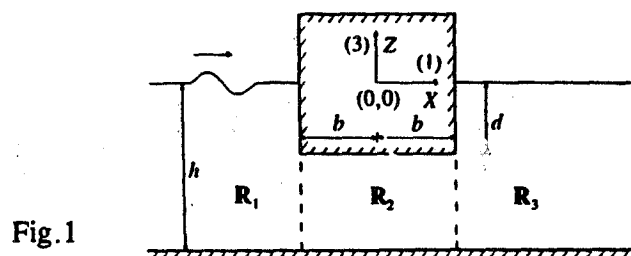


Fig. 1

The velocity potential  $\Phi$  at first ( $n=1$ ) and second order ( $n=2$ ) can be calculated from

$${}_n\Phi(x, z, t) = \operatorname{Re} \left[ \sum_{\beta} {}_n\phi_{\beta}(x, z) e^{-in\omega t} \right], \quad \beta = 0, 1, 3, 5, \quad n = 1, 2, \quad (1)$$

where  ${}_n\phi_{\beta}(x, z)$  is the spatial velocity potential associated with  $\beta$  mode of motion, and  $i = \sqrt{-1}$ .

The method of matched eigenfunction expansions is applied to obtain a solution. In order to use this method, three subdomains  $\mathbf{R}_l$ ,  $l = 1, 2, 3$ , are distinguished, and the spatial velocity potential  ${}_n\phi_{\beta l}$ ,  $l = 1, 2, 3$  is introduced so that:  ${}_n\phi_{\beta l} = {}_n\phi_{\beta}$  for  $(x, z) \in \mathbf{R}_l$ . The solution proceeds by taking eigenfunction expansions of the spatial velocity potential  ${}_n\phi_{\beta l}$  in each of the three subdomains and matching them at  $|x| = b$ . Equality of potentials and equality of their horizontal derivatives at  $|x| = b$ ,  $-h \leq z \leq -d$  are imposed as matching conditions.

An interesting feature in the solution was the development of significant second-order loads on a cylinder due to diffraction potential. This feature requires further investigation, so our attention from here on is focused on the diffraction potential  ${}_n\phi_{0l}$ .

The first-order solution,  ${}_1\phi_{0l}$ ,  $l = 1, 2, 3$ , may be written in the following form

$${}_1\phi_{01} = -\frac{ig}{\omega} \sum_{m=1}^{\infty} \left[ A_0 \delta_{1m} e^{-\alpha_m(x+b)} + R_{1m} e^{\alpha_m(x+b)} \right] \frac{\cos \alpha_{1m}(z+h)}{\cos \alpha_{1m}h}, \quad (2a)$$

$${}_1\phi_{02} = -\frac{ig}{\omega} \sum_{m=1}^{\infty} \left[ C_{1m}(1 - \delta_{1m} + \delta_{1m}x/b) e^{\mu_m x} + D_{1m} e^{-\mu_m x} \right] \cos \mu_m(z+h), \quad (2b)$$

$${}_1\phi_{03} = -\frac{ig}{\omega} \sum_{m=1}^{\infty} T_{1m} e^{-\alpha_m(x-b)} \frac{\cos \alpha_{1m}(z+h)}{\cos \alpha_{1m}h}, \quad (2c)$$

provided that

$$\frac{\omega^2}{g} = -\alpha_{1m} \tan \alpha_{1m}h : \mu_m = \frac{(m-1)\pi}{h-d}, \quad m \geq 1, \quad (2d,e)$$

where  $R_{11}$  and  $T_{11}$  are the amplitudes of the first-order reflected and transmitted wave, respectively,  $R_{1m}$  and  $T_{1m}$ ,  $m = 2, 3, \dots$ , are the amplitudes of the first-order evanescent modes,  $C_{1m}$  and  $D_{1m}$ ,  $m = 1, 2, \dots$ , are the coefficients determining the first-order potential in the subdomain  $\mathbf{R}_2$ , and  $\alpha_{1m} = \{-ik_1, \alpha_{12}, \alpha_{13}, \dots; k_1, \alpha_{12}, \dots > 0\}$ .

The first-order solution satisfies all of the boundary conditions except the matching conditions at first order. In order to satisfy the matching conditions and determine the unknown coefficients of the eigenfunction expansions, a matching procedure based on the method of matched eigenfunction expansions is applied. The procedure requires truncation of the eigenfunction expansions at some finite value  $m=M$  and leads to a set of simultaneous equations whose solution determines the coefficients of the eigenfunction expansions. The first order solution usually provides satisfactory results for  $M \leq 20$ .

The second-order solution,  ${}_2\phi_{0l}$ ,  $l = 1, 2, 3$ , may be written in the following form

$${}_2\phi_{01} = -\frac{ig}{2\omega} \sum_{j=1}^{\infty} R_{2j} e^{\alpha_j(x+b)} \frac{\cos \alpha_{2j}(z+h)}{\cos \alpha_{2j}h} \quad (3a)$$

$$\begin{aligned}
& -i\omega A_0^2 Q(\alpha_{11}, \alpha_{11}) e^{-2\alpha_{11}(x+b)} \frac{\cos 2\alpha_{11}(z+h)}{\cos^2 \alpha_{11}h} \\
& -2i\omega \sum_{m=1}^M A_0 R_{1m} Q(\alpha_{11}, -\alpha_{1m}) e^{-(\alpha_{11} - \alpha_{1m})(x+b)} \frac{\cos(\alpha_{11} - \alpha_{1m})(z+h)}{\cos \alpha_{11}h \cos \alpha_{1m}h} \\
& -i\omega \sum_{s=1}^M \sum_{m=1}^M R_{1s} R_{1m} Q(-\alpha_{1s}, -\alpha_{1m}) e^{(\alpha_{1s} + \alpha_{1m})(x+b)} \frac{\cos(\alpha_{1s} + \alpha_{1m})(z+h)}{\cos \alpha_{1s}h \cos \alpha_{1m}h}, \\
& {}_2\phi_{02} = -\frac{ig}{2\omega} \sum_{j=1}^{\infty} \left[ C_{2j}(1 - \delta_{1j} + \delta_{1j}x/b) e^{i\alpha_j x} + D_{2j} e^{-i\alpha_j x} \right] \cos \alpha_j(z+h), \quad (3b)
\end{aligned}$$

$$\begin{aligned}
& {}_2\phi_{03} = -\frac{ig}{2\omega} \sum_{j=1}^{\infty} T_{2j} e^{-\alpha_j(x-b)} \frac{\cos \alpha_j(z+h)}{\cos \alpha_j h} \quad (3c) \\
& -i\omega \sum_{s=1}^M \sum_{m=1}^M T_{1s} T_{1m} Q(\alpha_{1s}, \alpha_{1m}) e^{-(\alpha_{1s} + \alpha_{1m})(x-b)} \frac{\cos(\alpha_{1s} + \alpha_{1m})(z+h)}{\cos \alpha_{1s}h \cos \alpha_{1m}h},
\end{aligned}$$

provided that

$$Q(\alpha_{1s}, \alpha_{1m}) = \frac{\alpha_{1s}\alpha_{1m}}{4\omega^4/g^2} \frac{6\omega^4/g^2 + 4\alpha_{1s}\alpha_{1m} + \alpha_{1s}^2 + \alpha_{1m}^2}{4\omega^4/g^2 + (\alpha_{1s} - \alpha_{1m})^2}; \quad \frac{4\omega^2}{g} = -\alpha_{2j} \tan \alpha_{2j}h, \quad j=1, \quad (3d,e)$$

where  $R_{21}$  and  $T_{21}$  are the amplitude of the second-order reflected and transmitted wave, respectively,  $R_{2j}$  and  $T_{2j}$ ,  $j = 2, 3, \dots$ , are the amplitudes of the second-order evanescent modes,  $C_{2j}$  and  $D_{2j}$ ,  $j = 1, 2, \dots$ , are the coefficients determining the second-order potential in the subdomain  $R_2$ , and  $\alpha_{2j} = \{-ik_2, \alpha_{22}, \alpha_{23}, \dots; k_2, \alpha_{22}, \dots > 0\}$ .

The second-order solution, (3a) and (3c), consists of two main parts. The first part is associated with summation over  $j$  and satisfies the homogeneous form of the combined free-surface boundary condition, while the second part satisfies the nonhomogeneous form of the combined free-surface boundary condition. The first part in each equation consists of a propagating free-wave ( $j=1$ ) and evanescent components ( $j > 1$ ). The second part is a result of wave-wave, wave-evanescent mode, and evanescent mode-evanescent mode interactions.

The second-order solution satisfies all of the boundary conditions except the matching conditions at second order. The matching conditions are satisfied by applying the method of matched eigenfunction expansions. The method at second order requires truncation of the eigenfunction expansions at  $j=J$ . An analysis of the arguments of the cosine functions in (3) indicates that  $J \geq 2M - 1$ . Further calculations show that  $J = 2M - 1$  is sufficient, however, the second-order solution requires  $M > 20$  for waves of intermediate lengths.

The method of matched eigenfunction expansions can be applied to obtain the coefficient in (2) and (3) for various configurations. However, for a cylinder of substantial draft these coefficients can be obtained

analytically, so an analytical solution up to second-order is also made available.

#### 4. RESULTS

The solution obtained in the preceding Section has been used to calculate time-dependent components of pressure and loads.

Figures (2) show the modulus of pressure along the base of the cylinder ( $b/h=0.7625$ ,  $d/h=0.75$ ). The first-order pressure component ( $|_1p|$ ) and the second-order pressure component ( $|_2p|$ ) are presented for two dimensionless wave numbers. The presented theoretical results are obtained from the analytical solution.

The second-order components of pressure may become the dominant contributions to the loads in deep water. This is illustrated in Figures (3) where the ratio of the amplitude of the second-order component of the vertical force to the amplitude of the corresponding first-order quantity is plotted versus wave steepness ( $A_0k_1/\pi$ ). Experimental data in Fig. (3a) ( $b/h=0.4$ ,  $d/h=0.2$ ,  $k_1h=4.11$ ) and in Fig. (3b) ( $b/h=0.7625$ ,  $d/h=0.75$ ,  $k_1h=3$ ) confirms theoretical results.

Significant second-order load components have their origin in a relatively large second-order pressure component that occurs on the periphery of a cylinder. Figure (4) shows time series ( $T = 2\pi/\omega$ ) of the pressure underneath a cylinder ( $x/b=-0.931$ ; configuration as in Fig. 3b)) calculated by the method of matched eigenfunction expansions and measured in the wave flume. The theoretical pressure in Fig. (4) represents a sum of the first- and second-order time-dependent pressure components. The large second-order component in the time series is clearly visible even though the cylinder is exposed to waves of moderate steepnesses. ( $A_0k_1/\pi=0.034$ ).

Financial support has partially been provided by *Hydro-Alpha*, Poland and *Dynomar AB*, Sweden.

#### REFERENCES

Johansson, M. 1989 Barrier-type breakwaters. Thesis, Chalmers University of Technology, Göteborg.  
 Newman, J. N. 1990 Second-harmonic wave diffraction at large depths. *Journal of Fluid Mechanics*, 213, 59-70.  
 Sulisz, W. & Johansson, M. 1992 Second-order wave loading on a horizontal rectangular cylinder of substantial draught. *Applied Ocean Research*, 14, 333-340.

